

COMMISSIONING OF THE NON-INVASIVE PROFILE MONITORS FOR THE ESS LEBT

C.A. Thomas*, R. Tarkeshian, J. Etxeberria, S. Haghtalab, H. Kocevar,
N. Milas, R. Miyamoto, T. Shea,
European Spallation Source ERIC, Lund, Sweden

Abstract

In the Low Energy Beam Transport (LEBT) of the European Spallation Source (ESS) Linac, a specific Non-invasive Profile Monitor (NPM) has been designed to primarily monitor beam position monitor with 100 μm accuracy, and in addition enable beam profile and size measurement. We present the first measurement results using NPM during the commissioning of the LEBT. The measurement results conclude the beam position as well as the angle of the beam. The performance of the measurement is discussed and compared to the required accuracy for the position measurement. In addition, the profile of the beam along the propagation axis is reported, as measured for part or the full pulse transported in the LEBT. The fidelity of the reported profile will be discussed as function of the system sensitivity and image signal to noise ratio.

INTRODUCTION

The Non-invasive Profile Monitors in the ESS LEBT have been design to be primarily beam position monitors [1]. However, this instrument acquires an image of the residual gas fluorescence, and therefore it is capable of measuring the beam centroid angle, and the beam size as well [2]. In order to achieve the required accuracy, we have designed the instrument to be fiducialised, permitting the imaging system to be aligned on the beam reference axis within specified requirements. In this case, the accuracy of the beam position measurement is $\pm 100 \mu\text{m}$. The method to align the optical axis with the beam axis reference is described in the first section, together with the qualification measurements. Two NPMs, one for each transverse plane, have been installed in the Permanent Tank of the ESS LEBT, i.e. between the two solenoids of the LEBT. The commissioning of the LEBT has started in 2018, and continued through the first part of 2019. The NPMs were commissioned and the result of beam position measurement is presented and the accuracy and the precision of the measurement is discussed in the second session. In addition, it has been shown that the instrument is capable of measuring also the angle of the beam centroid. Processing the images to retrieve beam angles has been done successfully, and the performance on the measurement is shown and discussed also in the second section. Finally, the beam emittance can also be measured by fitting the beam size variation along the instrument longitudinal axis. Since the beam profile in the LEBT is not always Gaussian and also composed by a different species (mainly H^+ and H_2^+) the

beam emittance can be calculated only in a specific condition. In the last part of the second section, the results for emittance estimation based on Gaussian function are discussed. Finally, concluding remarks are drawn for the use of this diagnostic for the LEBT and the rest of the ESS linac.

INSTRUMENT QUALIFICATION

This NPM-LEBT is capable of measuring beam position by imaging the beam induced Fluorescence in the background gas. In order to have precise measurement precise setup of image magnification as well as knowledge of the image coordinates are required.

The NPM is equipped with a motorized lens, with an encoder to read out focusing position of the camera sensor with respect to the focal plane of the lens. Magnification m is given with the lens equation $m = X/F$, where X is the image sensor distance to the focal plane and F is the focal lens. The motor of the lens has limit switches to ensure the it is in the correct position. This introduces an additional offset that has to be determined.

The magnification at various lens positions are measured for all NPM units. Figure 1 shows measurements for one of the NPM units with a target positioned along the optical axis at various distances. In each position, the lens is adjusted and the target lens offset is found by minimizing the difference between the measured magnifications and the predicted ones using the lens equation with $X = \text{offset} + x_{\text{enc}}$. The minimization results in finding the offset with an average difference of less than 1%.

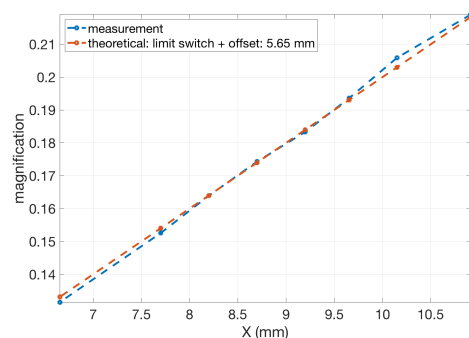


Figure 1: Magnification of the vertical unit of the first NPM set in the LEBT. Its focal length is $F = 50 \text{ mm}$.

The object coordinates relative to the image are given by the fiducialisation of the optical axis of the camera. The procedure consists in aligning the corner cube of the laser tracker in the centre of the image, and then recording several

* cyrille.thomas@ess.se

Content from this work may be used under the terms of the CC BY 3.0 licence (© 2019). Any distribution of this work must maintain attribution to the author(s), title of the work, publisher, and DOI

Table 1: Beam Position Systematic Error After Alignment for a Beam Positioned at $\pm 40\mu\text{m}$ in Both Axes

Unit	Working Distance (mm)	θ_{cam} (mrad)	Δ (mm)
Vertical	344.48	0.66	0.026
Horizontal	325.79	0.77	0.031

positions along the optical axis. Afterwards the camera can be positioned with its optical axis pointing to the beam reference axis. The precision of the alignment of the laser tracker corner cube is within 0.1 pixels, which corresponds to less than $5\mu\text{m}$. The laser tracker¹ accuracy is $15\mu\text{m}$. The overall uncertainty in positioning the optical axis of the camera is evaluated to be less than $50\mu\text{m}$ [1]. In addition, camera position is not exactly at the height reference. This implies the optical axis to meet the beam reference axis with an angle different from 90 degrees. This leads to a systematic error while measuring the beam position. The systematic error is the geometrical projection of the beam distance to the lens with respect to the nominal working distance to the optical axis. An example of reported error from alignment is shown in the Table 1. It shows that systematic error for a beam 40 mm from the centre in both axis would be less than $30\mu\text{m}$.

BEAM PARAMETERS FROM NPM IMAGE ANALYSIS

The NPM images contain information of the beam particles trajectories projected on either vertical or horizontal axis [2]. As such, information not only from the beam centre trajectory but also the beam size along the path can be retrieved from the images. An example of this analysis is shown in Fig. 2, which presents the image of the beam from the NPM unit measuring the vertical plane. On the image, profiles along the propagation axis z can be analyzed. In this example, the profiles are fit with a Gaussian function, from which the beam centre and rms width can be calculated. The result is a vector of beam position and size along the z -axis. With beam center measurements, the beam centroid position and angle can be extracted with a linear fit. This is shown in the figure by the red-diamonds dashed line. The beam size along the path can also be seen on the image. Here the rms values are shown as positive and negative values around the centers as yellow diamonds dashed lines. On the plot on the right, the mean projected profiles and the profile at the a given z -position are presented, together with the result of the Gaussian fit for the profile at the z -position. The profiles from the beam are not really Gaussian. In fact the model of the ion source and LEPT shows similar non-Gaussian distributions. Moreover, the model doesn't take into account the existence of H_2^+ particles, which has differ-

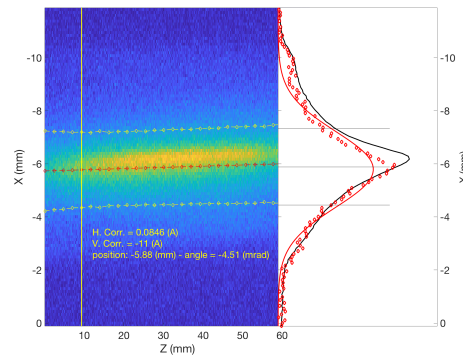


Figure 2: Image of the beam from the NPM vertical unit. The plot on the right shows the profile at the position $z = 9\text{ mm}$ (red diamonds), the Gaussian fit of this profile (red line), and the average profile over the image.

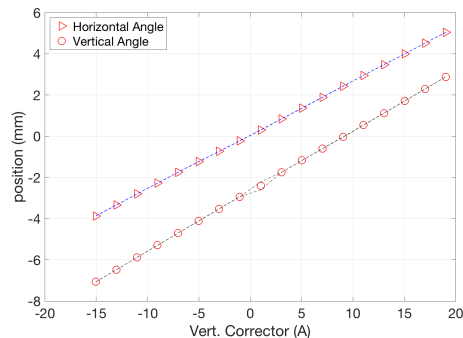


Figure 3: Beam position from the vertical and horizontal cameras of the NPM, as function of the vertical corrector magnet.

ent Twiss parameters than the protons and thus a different projected profile.

Beam Position Measurement

The beam position is extracted from the image analysis as shown in the Fig. 2. The Gaussian fit, in spite of the profile not been Gaussian returns a consistent and trustworthy value of the center of mass of the beam. The beam centre is measured from the centre of the image in both axis. Figure 3 presents the results of the beam position as function of the vertical corrector magnet current. On the figure, the reported points are the mean values of the measured centres and the dashed lines are the statistical rms variation for the a set of measurements. Note the r.m.s variation is too small to be distinguished. The beam is exiting the first solenoid in the LEPT, and the corrector magnets are locate inside the solenoid. As expected the relation is linear in both axis. However, the beam is not centered at the machines axis as an offset can be seen even when the correctors magnets ar turned off. Although not shown here, the same remarks can be done with the horizontal corrector scan. The accuracy of the measured position cannot be verified as no other beam position is available, however the position measured can be

¹ Leica Absolute Tracker AT960

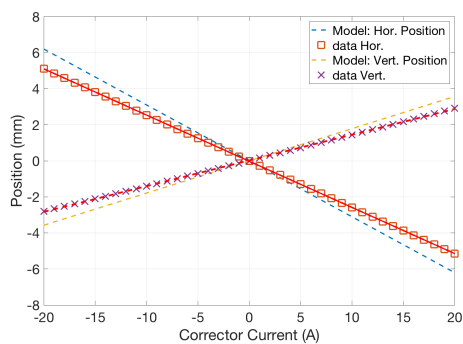


Figure 4: Relative beam position from the vertical and horizontal cameras of the NPM, as function of the horizontal corrector magnet and compared with our model prediction.

compared with our accelerator model. Figure 4 shows the result the relative beam position as observed by the NPM and compared to the model prediction. Here the beam position offset at zero correction is removed from the readings. To obtain full agreement between the model and the measurement, initial condition, i.e. the beam properties at the source have to be known as well as the misalignment of the focusing solenoid [3]. The data fit both position and angle of the beam at the NPM position. The agreement between the trend lines is within 20%. There are two possible explanations for this non-perfect matching. The first one is our poor calibration of the corrector field; it has been delivered with a single measurement point at maximum current, i.e. 120 A, so the field values at less than 10% of the max may not be entirely trustful. Also, hysteresis have been observed, which may also add to the modelling error.

The sensitivity of the measurement is represented by the statistical fluctuation of a set of measurements. It has been shown earlier [1] that it depends on the signal to noise ratio (SNR) on the images. Figure 5 compares the results of the statistical fluctuation of the position from a set measurements, and on which the SNR has been measured too, to the expected fluctuation values extracted from the Monte Carlo model presented in [1]. The trend shows a decrease of the error with increasing SNR, and the measured fluctuation is 5 μm larger than the predicted ones. In the model, the beam size is fixed, whereas in the measurement the beam size was varied by a factor larger than 5, and in doing this, the profiles are less Gaussian for larger beam sizes. This may explain the larger variation on the reported positions.

Beam Angle Measurement

The beam centroid angle is extracted from the vector of positions on the images as shown in the Fig. 2. The vector is fitted by a first order polynomial, and the angle is its differential coefficient. Figure 6 shows the measured angles of the beam along the same corrector scan as in the Fig. 3. On the figure, the same color codes are used. The mean angle values are reported as red diamond and circles for the horizontal and vertical axis, and the dashed lines show

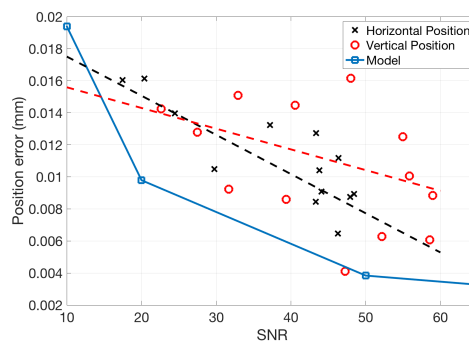


Figure 5: NPM position statistical fluctuation as measured on the vertical and horizontal cameras, as function of SNR.

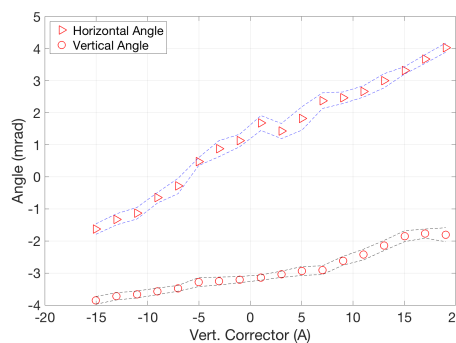


Figure 6: Beam angles from the vertical and horizontal cameras of the NPM, as function of the vertical corrector magnet.

the standard deviations of the measurements over a series of pulses with the same beam parameters. The precision of the measurement is shown in the Fig. 7. It shows the statistical fluctuation of the measurement as function of the SNR measured on the image. A comparison with the Monte Carlo simulation (blue line and squares) shows good agreement and the precision of the measurement to be less than 0.4 mrad for images with SNR > 50.

Similar to the position measurement, the accuracy of the measured angle cannot be measured directly. As above, the use of the accelerator model provides information on the model and on the accuracy of the measurement. Figure 8 presents the results of the angle measurement on the same horizontal scan as shown in Fig. 4. In the vertical plane, reported angles are linear as expected. The red line shows the result of a linear fit, and the magenta lines the 50% error uncertainty. The lines can't be distinguished from each other. The horizontal measured angles show a non-linear behaviour, following a main linear trend. The dash lines blue and gold report the predicted angles from our model, with the same initial condition as in the Fig. 4. Again, perfect agreement cannot be found. As discussed before, the linearity and strength of the corrector magnet in the operated range will have to be measured in order to understand the observed behaviour.

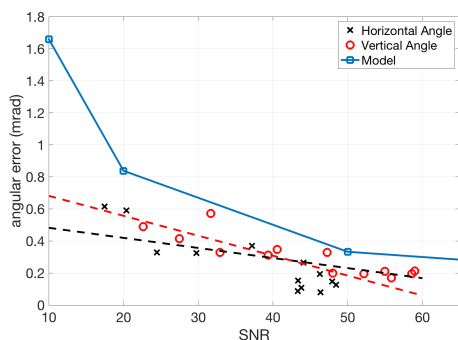


Figure 7: NPM angular error measurement on the vertical and horizontal cameras of the NPM, as function of SNR.

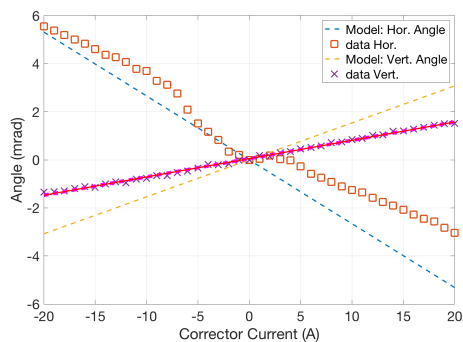


Figure 8: Beam angle from the vertical and horizontal cameras of the NPM, as function of the horizontal corrector magnet and compared with our model prediction.

Beam Emittance Measurement

From each image, the beam size along the trajectory z can be retrieved and thus the evolution of the beam size. Depending on the solenoid field strength, the beam either converges or diverges and the NPM location, which can be directly measured on the images. In addition, when the beam waist is on the image, its emittance can be calculated as shown in [2]. The quadratic fit of the square beam size trajectory has 3 parameters, which are linked to the emittance and to the Twiss parameters of the beam. When the beam waist is in the NPM field of view, the calculation of the emittance can be performed. An example is shown in the Fig. 9. The figure shows the square beam size trajectory, the quadratic fit and the calculated emittance. The average beam current is 70 mA peak, and the pulse is 6 ms long. The calculated emittance is $0.35 \pm 0.012 \pi$ mm mrad.

In order to verify this result, the beam emittance was measured with a dedicated instrument, an Alison Scanner, in the same condition, and reports 0.4π mm mrad. The agreement is within 12%.

CONCLUDING REMARKS

The NPMs have been commissioned in the LEBT. The measurement of the beam position in the ESS LEBT can

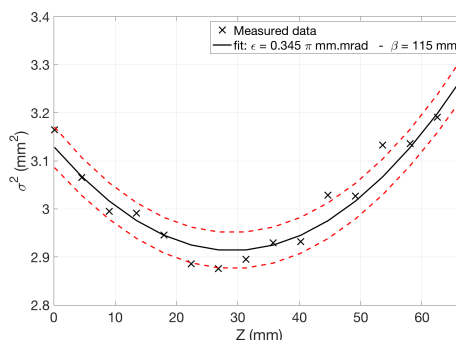


Figure 9: Square beam size trajectory. The line is a quadratic fit, and the dashed lines show the upper and lower 50% uncertainty interval from the fit. The calculated emittance is reported in the legend.

be performed with high precision, typically less than $10 \mu\text{m}$, and better than the 0.1 mm required accuracy. Beam position can be measured for each pulse delivered by the ESS ion source. The instrument can also measure the beam angle. The accuracy of the measurement depends on the image quality, and 0.4 mrad accuracy requires $\text{SNR} = 50$ or larger. It is also briefly shown that the measurement of the beam size trajectory can be used to measure the emittance of the beam. For accuracy, the measurement may require the beam to be focused at the NPM location. The comparison with standard emittance measurement with an Alison Scanner validates the NPM measurement. This will allow the use of the NPM to monitor the beam properties at the entrance of the downstream accelerator section, the RFQ, once a new pair of NPMs become available close to the RFQ entrance. At this position the NPM is also close to the beam waist and thus beam parameters such as position, angle and emittance, can be measured and monitored with sufficient accuracy to establish fast tuning of the RFQ.

REFERENCES

- [1] C.A. Thomas *et al.* “Design and Implementation of Non-Invasive Profile Monitors for the ESS LEBT”, in *Proc. of International Beam Instrumentation Conference (IBIC'16)*, Barcelona, Spain, Sept. 13-18, 2016, pp. 552–555. doi:10.18429/JACoW-IBIC2016-TUPG80
- [2] C.A. Thomas *et al.* “Design and Implementation of Non-Invasive Profile Monitors for the ESS LEBT”, In *Proc. 7th International Beam Instrumentation Conference (IBIC'18)*, Shanghai, China, 9-13 September 2018, pp. 455–458. doi:10.18429/JACoW-IBIC2018-WEPB12
- [3] N. Milas *et al.*, “Beam Based Alignment of Elements and Source at the ESS Low Energy Beam Transport Line”, presented at the 8th Int. Beam Instrumentation Conf. (IBIC'19), Malmö, Sweden, Sep. 2019, paper WEPP032, this conference.